Geomechanics and Engineering, *Vol. 26, No. 5 (2021) 499-512*
https://doi.org/10.12989/gae.2021.26.5.499

Experimental study of the evolution of pore water pressure and total stresses during and after the deposition of slurried backfill

El Mustapha Jaouhar[a], Jian Zheng* and Li Li[b]

Research Institute on Mines and Environment, Department of Civil, Geological and Mining Engineering
École Polytechnique de Montréal, C.P. 6079, succursale Centre-Ville, Montréal, QC, Canada H3C 3A7

(Received November 27, 2019, Revised July 26, 2021, Accepted September 8, 2021)

Abstract. Mining backfill is increasingly used in underground mines to fill stopes. Its successful application depends on the stability of barricades built to retain the backfill in stopes. The design of barricades requires a good estimation of pore water pressure (PWP) and total stresses during and after the deposition. On this regard, a large number of works have been published on analytical and numerical solutions. There are however very few experimental results with simultaneous measurements of PWP as well as horizontal and vertical total stresses that can be used to validate or calibrate the analytical and numerical solutions. For a specific project, field measurements are interesting in terms of representativeness to field conditions, but the results are very difficult to be correctly interpreted because the treated problem can involve a large number of uncertainties and the obtained results are due to combined effects of several influencing factors. Laboratory tests with simplified and well-controlled conditions are thus preferred. Until now, however, the most previous laboratory tests were conducted with dry backfill or with a tailings slurry instantaneously poured in a confining structure without simultaneous measurements of PWP as well as horizontal and vertical total stresses. Studies on the effects of filling rate and solid content of backfill on the variation of PWP and total stresses during the filling operation are absent. To fill these gaps, a series of column backfilling tests were conducted with simultaneous measurements of PWP as well as vertical and horizontal total stresses during and after the deposition of slurried backfill. When the filling rate is high, the test results showed that the PWP, horizontal and vertical total stresses increase at the same rate and equal to the iso-geostatic overburden pressure during the deposition of backfill slurry. Their peak values appear at the end of deposition. The backfill thus behaves like a liquid with little generation of effective stresses during the deposition. High filling rate and/or high solid content lead to high PWP and horizontal total stresses at the end of deposition. When the filling rate is small, the PWP and total stresses exhibit also peak values at the end of filling operation, but the vertical total stress at the center can continue increasing with time after the end of deposition due to the suspended sensor and occurrence of a phenomenon known as stress shielding effect. The results also showed that the settlement of settled backfill after the end of slurry deposition can generally exhibits a fast evolution rate stage, followed by a slow evolution rate stage. The duration of the fast evolution rate stage and the final settlement of the settled backfill increase as the solid content decreases. The final settlement after the end of slurry deposition is related to the solid content, not to the filling rate.

Keywords: **c**olumn tests; consolidation; mining backfill; pore water pressure; settlement; total stresses

1. Introduction

Mining backfill is commonly applied in underground mines worldwide as it can increase ore recovery, improve ground stability, and reduce mine dilution. By using mine wastes as backfill materials to fill underground mine stopes, the volume of surface disposal of mine wastes and minimize the associated environmental impact can be minimized (e.g., Grice 1998, Hassani and Archibal 1998, Benzaazoua *et al.* 2000, Aubertin *et al.* 2002, Bussière *et al.* 2004, Kesimal *et al.* 2004, Fall *et al.* 2004, 2005, Huynh *et al.* 2006, Darling 2011, Komurlu *et al.* 2016, Chen *et al.* 2018, Cao *et al.* 2018, 2021).

Upon the deposition of slurried backfill in a mine stope, excess pore water pressure (PWP) can instantaneously be generated first, due to the newly added backfill layers, and then progressively dissipated with the drainage. Depending on whether effective stresses are generated, the process of dissipation of excess PWP can be divided into sedimentation (without generation of effective stresses) and consolidation (with development of effective stresses) (Pedroni 2011, Li *et al.* 2013, Zheng *et al.* 2019, Qin *et al.* 2021a, 2021b). With the generation of effective stresses in the slurried backfill, arching effect associated with the shear stresses between the backfill and surrounding rock walls can develop, resulting in lower stresses in the slurried backfill than those based on overburden solution (Cui and Fall 2017). This phenomenon can be particularly pronounced with a low permeability backfill or/and small filling rate.

Understanding the evolution of PWP and total stresses associated with the self-weight consolidation during and

*Corresponding author, Postdoctoral fellow
E-mail: jian.zheng@polymtl.ca
[a]Ph.D. Candidate
E-mail: el.mustapha.jaouhar@gmail.com
[b]Professor
E-mail: li.li@polymtl.ca

ISSN: 2005-307X (Print), 2092-6219 (Online)

after the deposition of slurried backfill is critically important for design of barricade, a retaining structure built near the draw-point at the access drift of stope to hold the slurried backfill in place. Several cases of barricade failures have been reported in the past decades. The consequences varied from trapping of equipment, large economic loss to loss of lives (Bloss and Chen 1998; Sivakugan *et al.* 2006, 2014; Komurlu and Kesimal 2015; Yang *et al.* 2016). For instance, the failure of a barricade in Bronzewing Gold Mine in Western Australia resulted in the flooding of 18,000 m^3 slurried backfill into the working space and loss of three miners (Sivakugan 2008). It is thus a key aspect to have a full understanding of PWP and stresses in backfilled stopes and on barricades with the placement of slurried backfill. To this end, one can perform theoretical, numerical and experimental analyses on the variation of PWP and stresses in backfilled stopes and on barricades.

Over the years, a number of studies have been conducted to investigate the PWP and stresses in backfilled stopes through theoretical and numerical analyses (Askew *et al.* 1978, Aubertin *et al.* 2003, Li *et al.* 2005, Pirapakaran and Sivakugan 2007a, Li and Aubertin 2008, 2009, 2010, Fahey *et al.* 2010, Ting *et al.* 2011, 2012; El Mkadmi *et al.* 201,; Falaknaz *et al.* 2015a, b, c, Sobhi *et al.* 2017, Yang and Li 2017, Jahanbakhshzadeh *et al.* 2017, 2018a, 2018b; Jaouhar *et al.* 2018; Zheng *et al.* 2018a, b, Jaouhar and Li 2019, Zheng *et al.* 2019, Zheng *et al.* 2020a, b). These numerical and analytical solutions need to be validated by experimental results with simultaneous measurements of PWP as well as horizontal and vertical total stresses. The experimental work can be realized in field (Knutsson 1981; Belem *et al.* 2004; Helinski *et al.* 2011; Thompson *et al.* 2012; Doherty *et al.* 2015) or laboratory (Pirapakaran and Sivakugan 2007b; Ting *et al.* 2012). While the field measurements are very interesting in terms of representativeness to field conditions, but the results are very difficult to be correctly interpreted because the changes of PWP and total stresses can be due to the combined effects of several influencing factors such as the drainage and consolidation of backfill, cement hydration and desiccation, seepage through the joint network in the rock mass walls, wall closures associated with neighboring excavation or/and creep of rock, etc. The measured results are thus very useful for the design of barricades of a specific project at the studied mine, but less helpful for understanding the effects of each individual influencing factor on the variation of PWP and total stresses. In addition, field measurements suffer from several uncertainties, including irregular geometry of stopes, temperature, movement of rock walls, mechanical and hydraulic properties of the confining rock mass walls, contact conditions between the backfill and confining walls, dynamic loading induced by nearby blasting, etc. The calibration of PWP, stress and temperature sensors can usually be done on the surface, rarely in underground stopes after their installation in the stopes. Interpreting the field measurements results can thus be very challenging with a number of uncertainties. All these limitations are closely related to the access restriction in the stopes. These limitations do not apply in laboratory tests, in which one can have better control or measurement of testing conditions and backfill properties. Calibration of testing instruments (PWP and stress sensors) can be done before and after every backfilling test (Take and Valsangkar 2001; Pirapakaran and Sivakugan 2007b; Li *et al.* 2014). The results interpretation is more straightforward than field measurements. Laboratory tests are thus preferred for better understanding the effects of each individual influencing factor on the variation of PWP and total stresses in backfilled stopes.

Take and Valsangkar (2001) conducted centrifuge tests in laboratory to measure the horizontal earth pressure on retaining walls. Only the horizontal stress was measured. Pirapakaran and Sivakugan (2007b) conducted backfilling tests in columns. Only the mean of vertical stress over the bottom of the columns was measured. Li *et al.* (2014) conducted backfilling tests in a silo to simulate a mine stope, both the horizontal and vertical stresses were measured, but only at the center with the horizontal and vertical stress sensors located at different elevations. All these laboratory tests were realized with dry backfill. The simultaneous measurements of PWP and total stresses were absent.

Over the years, one sees also the publications of a few laboratory tests with tailings slurry. Pedroni (2011) conducted sedimentation and self-weight consolidation tests in a column filled with a tailings slurry. The tailings were poured in the column. Only the PWP was measured after the deposition. Essayad and co-worker (Essayad 2015; Essayad and Aubertin 2021) conducted column consolidation tests with tailings under different vertical loadings. PWP was measured with the measurement of total stresses inside the tailings. Saleh-Mbemba and Aubertin (2018) investigated the consolidation behavior of tailings slurry poured in a large box. Only PWP was measured. All these tests were realized with a given solid content tailings slurry quickly poured in a confining structure. The measurements of vertical and horizontal total stresses were absent.

To fill this gap and better understand the self-weight consolidation characteristics of slurried backfill during and after the deposition, a series of laboratory tests have been conducted in an instrumented column. The backfill was poured in the column at a controlled pace. The PWP, vertical and horizontal total stresses near the bottom of the column as well as the settlement of the tailings-water interface were measured during and after the deposition. The influence of solid content and filling rate on the evolution of PWP, total stresses and settlement were investigated. The evolution of void ratio and consolidation coefficient were evaluated.

2. Test material

The tailings used in this study were taken from a hard rock mine in Quebec province, Canada. The tailings have a specific gravity of Gs = 2.74. Fig. 1 shows the grain-size distribution curve of the tested tailings with a uniformity coefficient of Cu = 11, and curvature coefficient of Cc = 1.08.

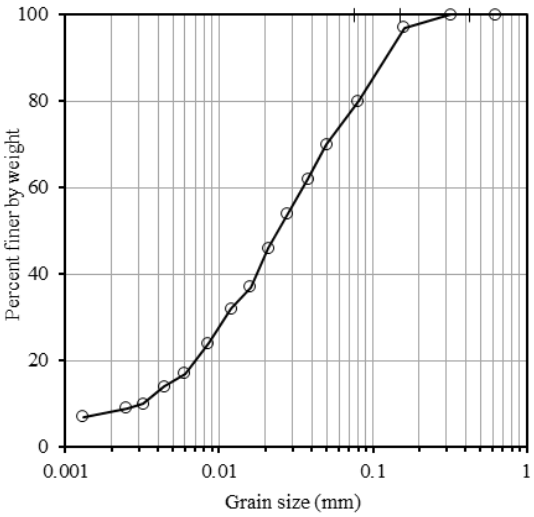

Fig. 1 Grain size distribution of the tested tailings (Boudrias 2018)

Table 1 The physical properties of the tested slurried backfill

Case	0	1	2	3	4	5
Targeted solid content (%)	68	68	68	62.5	72.5	72.5
Obtained solid content (%)	67.76	68.26	67.97	61.00	72.52	72.26
Water content (%)	47.58	46.49	47.14	63.94	37.90	38.38
Density (g/cm^3)	1.76	1.77	1.74	1.65	1.82	1.84
Unit weight (kN/m^3)	17.30	17.33	17.04	16.17	17.82	18.02
Void ratio	1.27	1.25	1.30	1.69	1.06	1.04

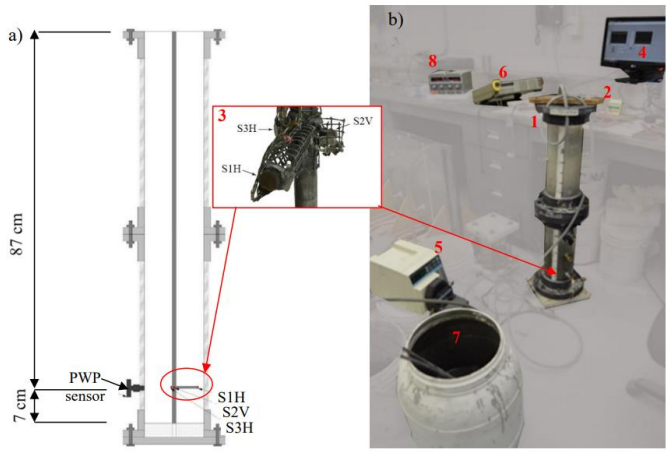

Fig. 2 A schematic (a) and photographical (b) presentation of the test instrumentation: (1) column; (2) amplifier; (3) miniature stress sensors; (4) data acquisition system; (5) pump; (6) multimeter; (7) tailings bucket; (8) power supply

The slurried backfill were prepared by placing a given mass of dry tailings in a bucket and mixing with tap water to the targeted solid contents of 62.5, 68, and 72.5%. Later, water content was measured and the final solid contents of the tested slurried backfill ranges from 61.0 to 72.52%. Table 1 shows the physical properties of the tested slurried backfill, including the water content, density, unit weight, and void ratio of each solid content backfill. It can be seen that the obtained solid contents are slightly different than the targeted ones.

3. Structural reliability analysis

Fig. 2 shows a schematic diagram (Fig. 2(a)) and a picture (Fig. 2(b)) of the test instrumentation. The column is made of Plexiglas, which is 1 m high and has an inner diameter of 0.15 m. A PWP sensor (Omega pressure sensor ® PX243) was installed at a position 7 cm above the bottom of the column. It was kept saturated and covered with a saturated filter to prevent the conglomeration associated with the movement of fine particles. Three miniature stress sensors (TML PDA-200kPa) were installed at the same elevation as the PWP sensor to measure the horizontal (S1H

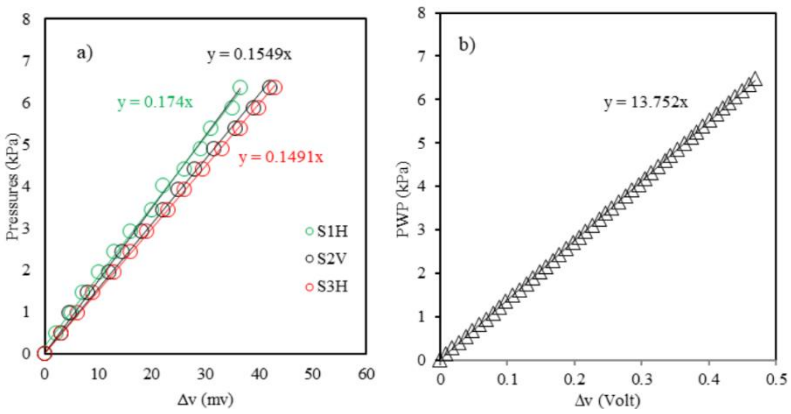

Fig. 3 Calibration curves of stress (a) and PWP (b) sensors

Table 2 Testing program of column backfilling

Cases	Filling rate (m/h)	Solid content (%)
0 (reference)	0.18	68
1	0.83	68
2	0.11	68
3	0.19	62.5
4	0.23	72.5
5	0.17	72.5

and S3H) and vertical (S2V) total stresses. They have a radius of 0.5 cm and a thickness of 0.2 cm. The three stress sensors were installed on two cages, which were fixed on a stiff rod placed in the center of the column. Sensor S1H was placed 5.5 cm from the center of the rod, facing vertically to measure the horizontal total stress. Sensor S2V was placed near the rod with the face upward to measure the vertical total stress. Sensor S3H was placed 1 cm from the center of the rod with the face parallel to the rod to measure the horizontal total stress.

The input voltage for the PWP sensor was 8 volts and the output voltage was recorded by the data acquisition system. The input voltage for the stress sensors was 2 volts and the output voltage was amplified by an amplifier and then measured by a multimeter.

The PWP and stress sensors were calibrated before each test by filling water in the column to different levels. Fig. 3 shows the calibration curves of the stress and PWP sensors. The slopes of the straight lines were used to back calculate the measured PWP and total stresses.

The prepared slurried backfill was stored in a bucket and continuously mixed with a portable mixer to minimize the possible segregation. The column filling operation was performed with a pump to ensure a constant filling rate. Table 2 shows the realized testing program. Three filling rates were tested for the slurried backfill of 68%. To investigate the influence of solid content on the drainage and consolidation behavior, a filling rate of 0.18 m/h was targeted but not entirely reached due to the difficulty in controlling the pumping rate.

Table 2 shows the realized testing program. Three filling rates were tested for the slurried backfill having a solid content by mass of 68%. To investigate the influence of solid content on the drainage and consolidation behavior, a filling rate of 0.18 m/h was targeted but not entirely reached due to the difficulty in controlling the pumping rate.

4. Test results and interpretation

4.1 Evolution of the PWP, vertical and horizontal total stresses during and after the deposition

Fig. 4 shows the evolution of the PWP, vertical and horizontal total stresses during and after the deposition of the slurried backfill of 68% solids by mass when the filling rates are 0.18 (Case 0, Fig. 4a), 0.83 (Case 1, Fig. 4b) and 0.11 m/h (Case 2, Fig. 4c), respectively. One sees that the PWP, horizontal and vertical total stresses continuously increase during the deposition for all the three cases. For case 1 with a filling rate of 0.83 m/h (Fig. 4b), the PWP, horizontal and vertical total stresses increase at the same rate and equal to the iso-geostatic overburden pressure during the deposition. These results indicate that the slurried backfill behaves like a heavy liquid without any effective stress generated during the deposition. Similar results have been reported with field measurements (Helinski *et al.* 2011, Thompson *et al.* 2012). When the filling rate is decreased to 0.18 m/h (Case 0, Fig. 4a), one can note slight difference between the PWP and the vertical and horizontal stresses during the slurry deposition, indicating slight occurrence of drainage and consolidation during the filling operation. When the filling rate is further reduced to 0.11 m/h (Case 2, Fig. 4(c)), the PWP, horizontal and vertical total stresses deviate each other with the vertical total stress near the center higher than the horizontal total stresses near the center and wall during the filling operation. Before the end of filling operation, the PWP has become much lower than the vertical and horizontal total stresses, indicating the development of effective stresses.

After the end of fast deposition (Case 1, Fig. 4(b)), the PWP decreases at almost the same rate as the horizontal and vertical total stresses until the end of the test, indicating little generation of effective stresses after the end of deposition. These results are straightforward. With high filling rate, the time of the dissipation of excess PWP during

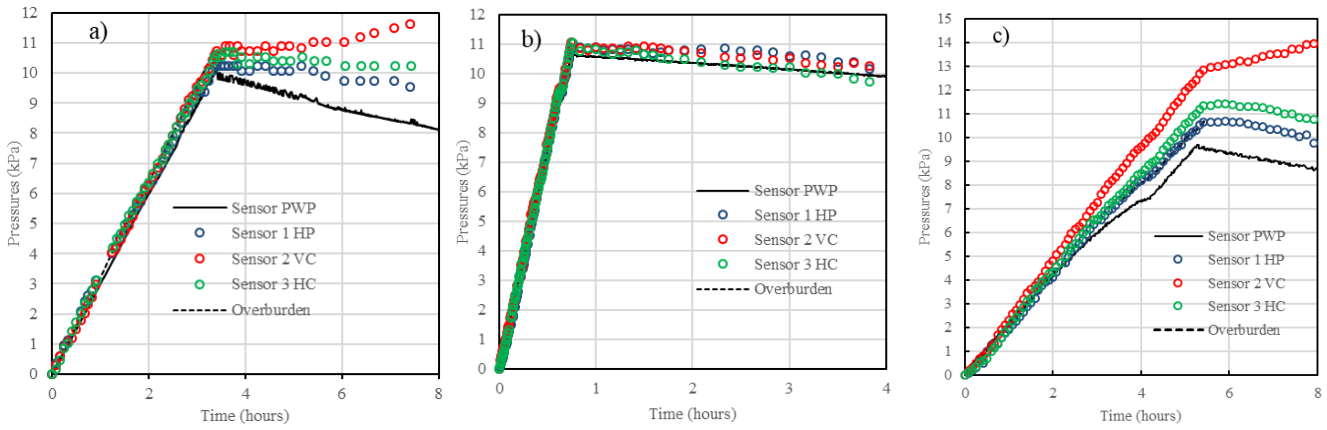

Fig. 4 Evolution of the PWP, vertical and horizontal total stresses during and after the deposition of the slurried backfill of 68% solids by mass when the filing rates are 0.18 (a, Case 0), 0.83 (b, Case 1) and 0.11 m/h (c, Case 2), respectively

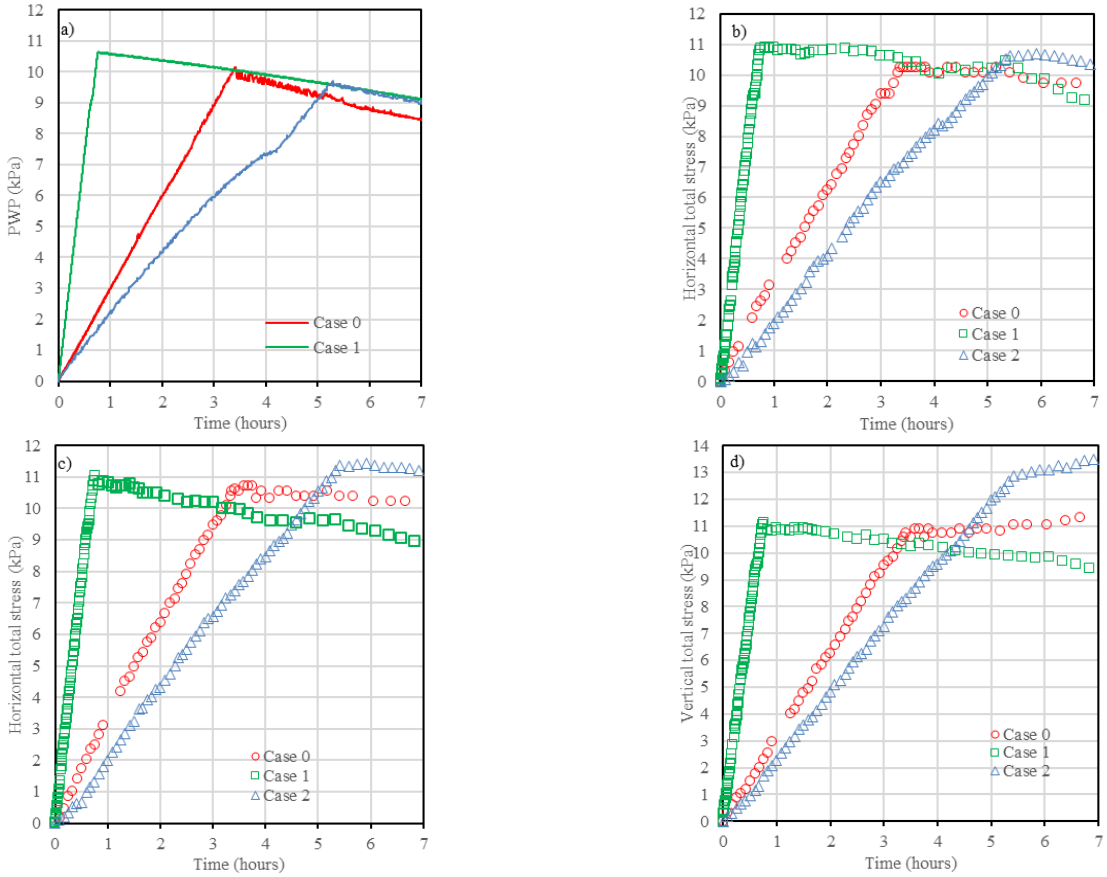

Fig. 5 Evolution of the PWP (a), horizontal total stresses near the wall (b) and the center (c), and vertical total stress near the center (d) of the column when the solid content is 68% and the filling rates are 0.18 (Case 0), 0.83 (Case 1), and 0.11 m/h (Case 2), respectively

the deposition is short, resulting in high excess PWP at the end of deposition, which needs long time to be dissipated. When the filling rates are small (Case 0, Fig. 4(a); Case 2, Fig. 4(c)), drainage and consolidation have taken place during the deposition of slurry. After the end of slurry deposition, the drainage and consolidation become pronounced. The horizontal total stresses and PWP decrease with time. Again, similar results have been reported with field measurement (Thompson *et al.* 2012). The deviation between the PWP and the horizontal and vertical total stresses indicates an increase of effective stresses.

It is however noted that the vertical total stresses in cases 0 (Fig. 4(a)) and 2 (Fig. 4(c)) keep increasing and even become higher than the iso-geostatic overburden pressure after the end of deposition. This counterintuitive result is probably due to a phenomenon known as stress shielding (Selig 1980, Clayton and Bica 1993, Talesnick 2005, Berthoz *et al.* 2013), which will be further addressed

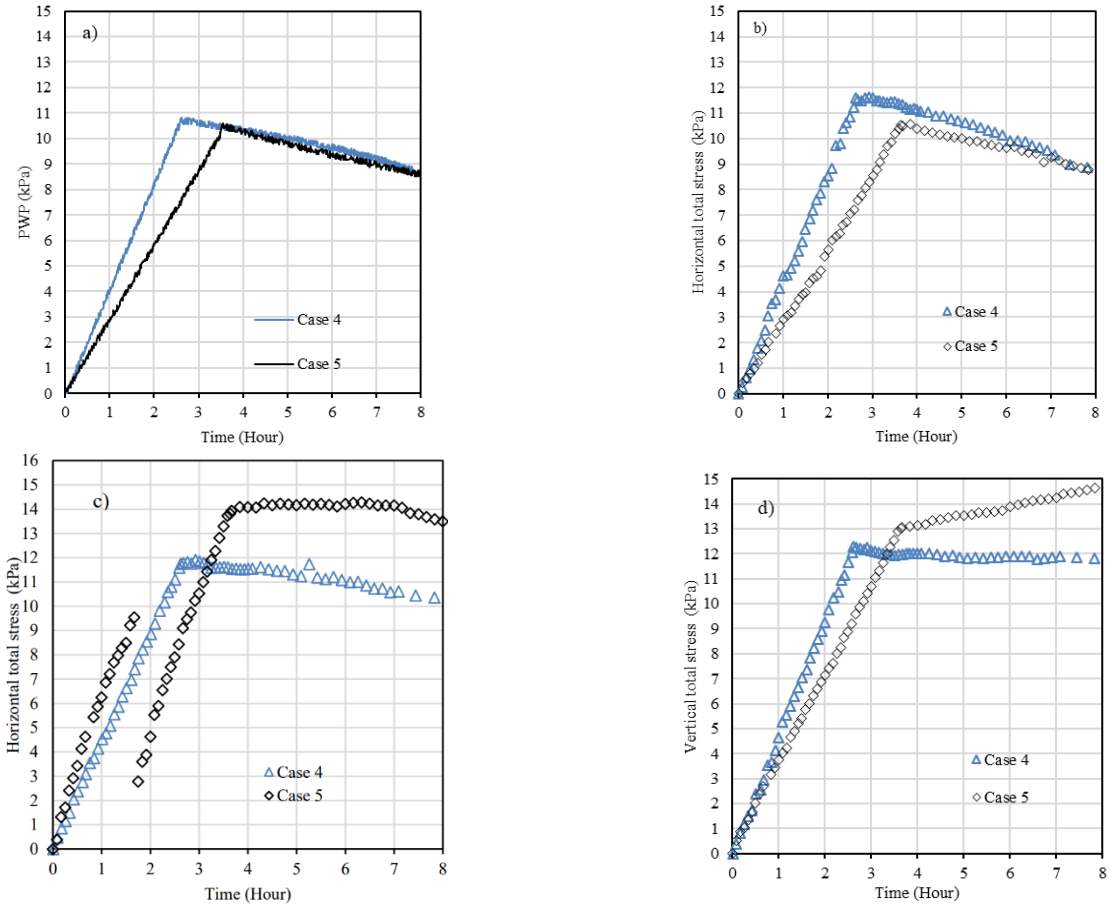

Fig. 6 Evolution of the PWP (a), horizontal total stresses near the wall (b) and the center (c), and vertical total stress near the center (d) of the column when the solid content is increased to 72.5% while the filling rates are 0.23 m/h (Case 4) and 0.17 m/h (Case 5), respectively

in the section "Discussion".

To further and better elucidate the influence of filling rate on the evolution of the PWP and stresses, the results shown in Fig. 4 are reorganized and presented in Fig. 5 for the evolution of the PWP (Fig. 5(a)), the horizontal total stresses near the wall (Fig. 5(b)) and the center (Fig. 5(c)), and the vertical total stress near the center (Fig. 5(d)) of the column during and after the deposition when the solid content is 68% and the filling rates are 0.18 (Case 0), 0.83 (Case 1), and 0.11 m/h (Case 2), respectively. It can be seen that high filling rate results in high PWP at the end of deposition, with the highest peak PWP in the fastest filling (Case 1 with 0.83 m/h) and lowest peak value of PWP in the slowest filling (Case 2 with a filling rate of 0.11 m/h). These results indicate again the importance of taking into account the influence of drainage and consolidation during the deposition to obtain accurate evaluation of the PWP in backfilled stopes and on barricades. Similarly, the vertical and horizontal total stresses at the end of slurry deposition are slightly lower in Case 0 than those in Case 1, indicating again the importance of taking into account the influence of drainage and consolidation during the deposition to obtain accurate assess of the total stresses in backfilled stopes for barricade design. These results indicate that fast backfilling should be avoided to prevent the generation of high horizontal total stress on barricades. However, when the filling rate is further reduced to 0.11 m/h in Case 2, the resulted vertical and horizontal total stresses near the center at the end of slurry deposition become higher than those resulted from high-speed filling in Cases 0 and 1. In addition, one notes that the vertical total stresses in Cases 0 with filling rate of 0.18 m/h and Case 2 with filling rate of 0.11 m/h keep increasing with time even after the end of slurry deposition. These somehow strange results are probably related to a phenomenon, called stress shielding (Selig 1980, Clayton and Bica 1993, Talesnick 2005, Berthoz *et al.* 2013). This aspect will further be addressed in the section "Discussion".

Similar results have been observed and shown in Fig. 6 when the solid content is increased to 72.5% while the filling rates are 0.23 m/h (Case 4) and 0.17 m/h (Case 5), respectively. Smaller PWP and horizontal total stress resulted from slower filling operation. When the filing rate is small, high vertical total stress develops at the end of slurry deposition, which continues increasing even after the end of slurry deposition, probably due to stress shielding development (Selig 1980, Clayton and Bica 1993, Talesnick 2005, Berthoz *et al.* 2013). This will be further addressed in "Discussion". In addition, the horizontal total stress of Case 5 is very unstable with discontinuity reading despite no anomaly was observed on the sensor (S1H).

Fig. 7 shows the evolution of the PWP, vertical and

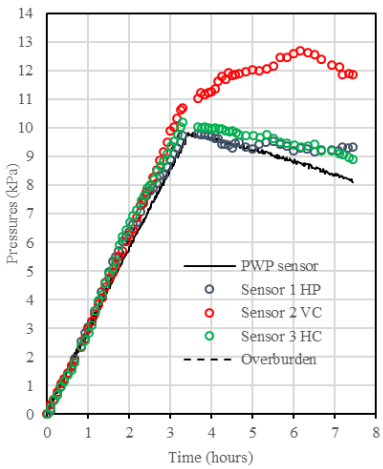

Fig. 7 Evolution of the PWP, vertical and horizontal total stresses when the solid content is reduced to 62.5% (Case 3) with a filling rate of 0.19 m/h

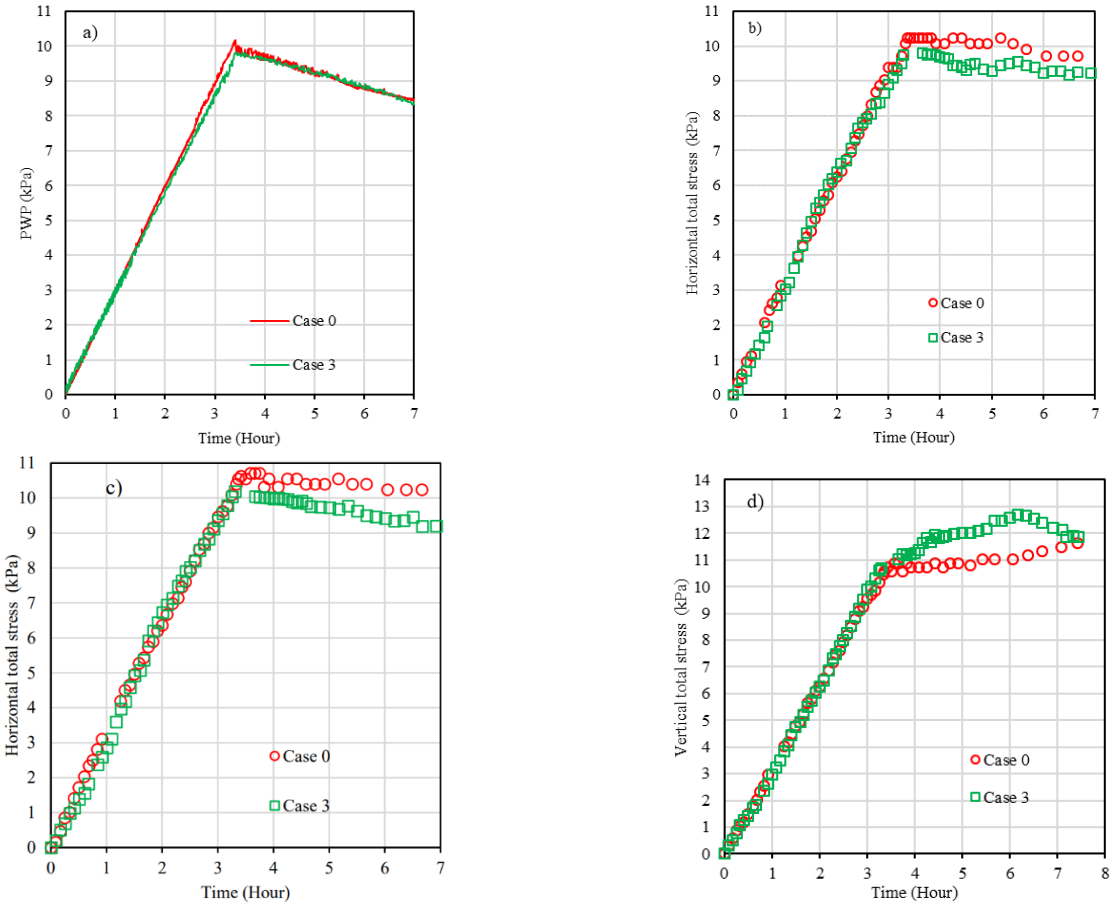

Fig. 8 Evolution of the PWP (a), horizontal total stresses near the wall (b) and the center (c), and vertical total stress near the center (d) of the column when the filling rates were tried to keep around 0.18 m/h and the solid contents are 68 (Case 0 with a filling rate of 0.18 m/h) and 62.5% (Case 3 with a filling rate of 0.19 m/h), respectively

horizontal total stresses during and after the deposition of slurried backfill when the solid content was reduced to 62.5% while the filling operation was performed at a filling rate of 0.19 m/h, even effort was made to try obtaining a value close to 0.18 m/h used in the reference case (Case 0). One can see that the horizontal and vertical total stresses almost increase at the same rate and close to the iso-geostatic overburden pressure during the deposition. The PWP are however slightly lower than the horizontal and vertical total stresses, indicating slight occurrence of arching effect. In addition, one notes that the peak values of the horizontal total stresses and PWP at the end of deposition are slightly smaller than those of Case 0 (Fig. 4(a)) because the density and unit weight of the slurried

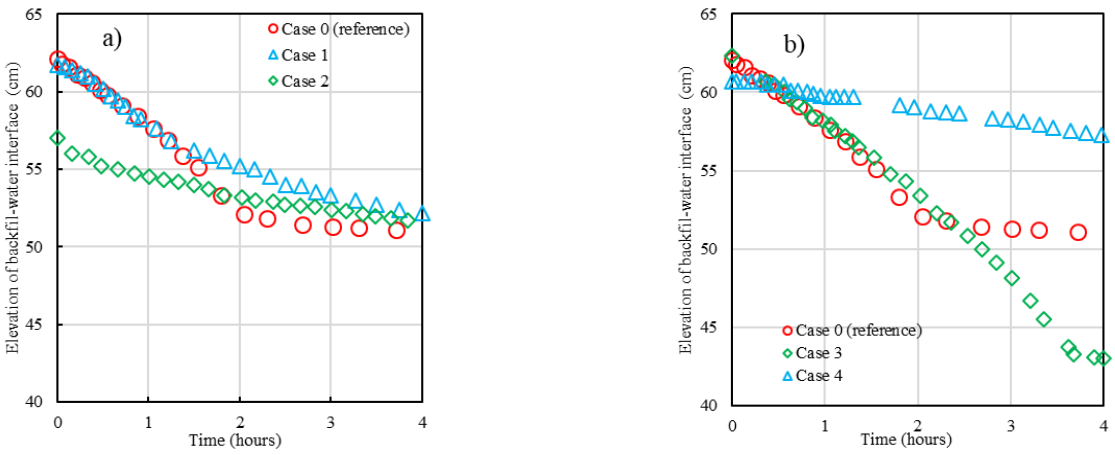

Fig. 9 Evolution of the backfill-water interface elevations after the end of slurry deposition: (a) when the solid content is 68% while the filling rates are 0.18 (Case 0), 0.83 (Case 1) and 0.11 m/h (Case 2), respectively; (b) when the filling rate was tried to be kept constant around a value of 0.18 m/h while the solid contents are 68 (Case 0 with a filling rate of 0.18 m/h), 62.5 (Case 3 with a filling rate of 0.19 m/h) and 72.5% (Case 4 with a filling rate of 0.23 m/h), respectively

backfill of 62.5% are smaller than those of Case 0 (see Table 1). After the end of deposition operation, the horizontal total stresses and PWP decrease with time. These results along with those shown in Fig. 4 indicate that the most critical moment for barricade design is the end of deposition because the stability of barricades mainly depends on horizontal total stress. One sees again a counterintuitive increase of the vertical total stress after the end of deposition; this aspect will further be addressed in the section “Discussions”.

To further and better illustrate the influence of the solid content on the evolution of the PWP and stresses, the results shown in Figs 4 and 7 are reorganized and presented in Fig. 8 for the evolution of the PWP (Fig. 8(a)), horizontal total stress near the wall (Fig. 8(b)) and the center (Fig. 8(c)), and vertical total stress near the center (Fig. 8(d)) of the column during and after the deposition when the filling rates were tried to keep constant and the solid contents are 68 (Case 0 with a filling rate of 0.18 m/h) and 62.5% (Case 3 with a filling rate of 0.19 m/h), respectively.

Despite the slight difference in the filling rates, the results generally show higher PWP, vertical and horizontal total stresses at the end of slurry deposition with higher solid content. Finally, one sees again the counterintuitive increase of the vertical total stress after the end of slurry deposition in Case 3 (Fig. 8(d)) due probably to the stress shielding effect (Selig 1980, Clayton and Bica 1993, Talesnick 2005, Berthoz *et al.* 2013).

4.2 Evolution of consolidation parameters during and after the deposition

During and after the slurry deposition, drainage and consolidation take place. Draining water flows upward and forms a pond. An interface between the pond and the settled backfill forms. The measurement of the settlement of the backfill-water interface can be useful to estimate some hydraulic property parameters.

Fig. 9(a) shows the evolution of the backfill-water interface elevations after the end of slurry deposition when the solid content is 68% while the filling rates are 0.18 (Case 0), 0.83 (Case 1) and 0.11 m/h (Case 2), respectively. It is very difficult to understand and explain how filling rate affects the evolution rate of the backfill-water interface settlements of the same solid content. In general, one can see that the backfill-water interfaces of the three cases moved downward after the end of slurry deposition due to dissipation of excess PWP and expulsion of pore water. One can see also that the backfill-water interface first shows a fast settlement, followed by a slow settlement stage. When the filling rate is very small (Case 2 with a filling rate of 0.11 m/h), significant drainage and consolidation took place during the filling operation, resulting in significant settlement and low level elevation of backfill-water interface at the end of slurry deposition. The further drainage and consolidation after the end of slurry deposition resulted in a small settlement of 5.3 cm. When the filling rate is higher than 0.11 m/h, the drainage and consolidation during the filling operation can be small, resulting in small settlement and high level elevation of backfill-water interface at the end of slurry deposition. The further drainage and consolidation after the end of slurry deposition resulted in large settlements (11 cm for Case 0 and 9.5 cm for Case 1). Finally, it is interesting to note that the backfill-water interfaces of the three cases reach the same position around 4 hours after the end of slurry deposition. This tends to indicate that the filling rate does not influence the final settlement of the backfill.

Fig. 9(b) shows the evolution of backfill-water interface elevations after the end of slurry deposition when the filling rate was tried to be kept constant around a value of 0.18 m/h while the solid contents were 68% (Case 0 with a filling rate of 0.18 m/h), 62.5% (Case 3 with a filling rate of 0.19 m/h) and 72.5% (Case 4 with a filling rate of 0.23 m/h), respectively. When the solid content is higher than 62.5% (Case 4), one only sees a slow evolution stage of the backfill-water interface while the fast evolution rate stage is absent. The settlement of the final backfill-water interface is quite small. When the solid contents are smaller than 72.5% (Case 3 with a solid content by mass of 62.8% and Case 0

with 68%), two evolution rate stages appear in the backfill-water interface. The duration of the fast evolution rate and settlement of the final backfill-water interface increase as the solid content decreases. These results indicate that it is advantageous to thicken the tailings or backfill if one target to accelerate the drainage and consolidation of slurried materials.

Having the measurements of PWP, total stresses and settlements, some hydraulic property parameters can be estimated. For instance, the void ratio e_i at a given time t_i after the end of slurry deposition can be calculated as follows:

$$e_i = e_{end} - \frac{\Delta hi}{h_{end}} \ (1 + e_{end}) \tag{1a}$$

where h_{end} (m) is the thickness of the settled backfill at the end of slurry deposition; Δh_i (m) is the settlement of the backfill-water interface at the given time t_i after the end of slurry deposition; e_{end} is the void ratio of the settled backfill at the end of slurry deposition, determined as follows:

$$e\_end = h\_end/h\_0 \quad (1 + e\_0\ ) - 1 \tag{1b}$$

where h_0 (m) is total thickness of the poured slurried backfill (including the water pond on top of the settled backfill); e_0 is the initial void ratio of slurred backfill, calculated as follows:

$$e_0 = \frac{\rho_s}{\rho_w} \ \left(\frac{1}{P} - 1\right) \tag{1c}$$

where ρ_s (kg/m^3) and ρ_w (kg/m^3) are the densities of solids and water, respectively; P is the solid content by mass of the slurried backfill.

In this study, two manners of evaluating the coefficient of consolidation c_v have been used. The first one is to use the measured vertical total stress and PWP to obtain the vertical effective stress (called measured vertical effective stress) at the given time t_i after the end of slurry deposition, which can be calculated as follows:

$$\sigma'_{i\_m} = \ \sigma_i - u_i \tag{2}$$

where u_i and σ_i are the measured PWP and vertical total stress, respectively, at the point of calculation at the given time t_i after the end of slurry deposition.

The second manner is to roughly estimate the vertical effective stress by neglecting the possible development of the arching effect. The estimated vertical effective stress at the given time t_i after the end of slurry deposition is then expressed as follows:

$$\sigma'_{i\_e} = \ \gamma_w h_{wi} + \gamma_i (H_0 - h_{wi}) - u_i \tag{3}$$

where H_0 (m) is the height between the top surface of the water pond and the point of calculation (and PWP measurement) at the end of slurry deposition; h_{wi} (m) is the thickness of the water pond on the top surface of the settled backfill at the given time t_i after the end of slurry deposition; γ_w (kN/m^3) is the unit weight of water; γ_i (kN/m^3) is the unit weight of the slurried backfill at the given time t_i after the end of slurry deposition, which can be calculated as follows:

$$\gamma_i = \gamma_w \frac{G_s - e_i}{1 + e_i} \tag{4}$$

where Gs is the specific gravity of the slurried backfill.
The coefficient of compressibility $a_{v,i}$ (1/kPa) can then be calculated as follows:

$$a_{v,i} = \frac{e_1 - e_i}{\sigma'_i - \sigma'_1} \tag{5}$$

where e_1 and e_i are the void ratios of the settled backfill corresponding to the effective stress of σ'_1 and σ'_i, respectively.

The hydraulic conductivity k_i at time t_i after the end of slurry deposition can be estimated as fallows based on Darcy's law:

$$k_i = \frac{Q_i}{A} \frac{\Delta L_i}{\Delta H_i} \tag{6}$$

where Q_i (m^3/s) is the flow rate of the draining water at time t_i after the end of slurry deposition; A (m^2) is the cross-section area of the column; ΔH_i (m) and ΔL_i (m) are the difference of hydraulic heads and thickness between the PWP and stress measurement point near the bottom of the column and the backfill-water interface, respectively.

The consolidation coefficient $c_{v,i}$ of the settled backfill at time t_i after the end of slurry deposition can then be calculated as follows:

$$c_{v,i} = \frac{k_i \times (1 + e_i)}{a_{v,i} \times \gamma_w} \tag{7}$$

where γ_w (kN/m^3) is the unit weight of water.

Fig. 10 shows the variation of the void ratio (Fig. 10a) and coefficient of consolidation c_v (Fig. 10b) as a function of estimated effective stress after the end of slurry deposition for Cases 0, 1 and 2. The variation of the void ratio (Fig. 10(c)) and coefficient of consolidation c_v (Fig. 10(d)) as a function of the effective stress based on the measured vertical total stress and PWP for the three cases is also plotted. It can be seen that the void ratio decreases as the estimated effective stress increases. These results are straightforward. As the drainage and consolidation take place, pore water tends to be expelled, resulting in a decrease of void ratio. One can also see that Cases 0 and 2 show similar consolidation curves (e-logσ'), which are higher than that of Case 1. This result is counterintuitive because the used tailings and solid contents are identical for the three cases and the consolidation curves of the three cases are expected to be identical for the three cases. As the only difference between Case 1 and Cases 0 and 2 is in their filling rates (0.83 m/h in the former case; 0.18 and 0.11 m/h in the two latter cases), the problem is probably related to the vertical effective stress estimation by considering the vertical total stress equaling to the iso-geostatic overburden pressure (see Eq. 3). The neglect of the arching effect may result in an overestimate of the effective stress, especially when the filling rate is small for Cases 0 and 2. Another possible reason is the implicit assumption of homogenous settled backfill along the whole height while the settled backfill is probably not homogenous due to the drainage and consolidation and associated segregation (Dalcé *et al.*

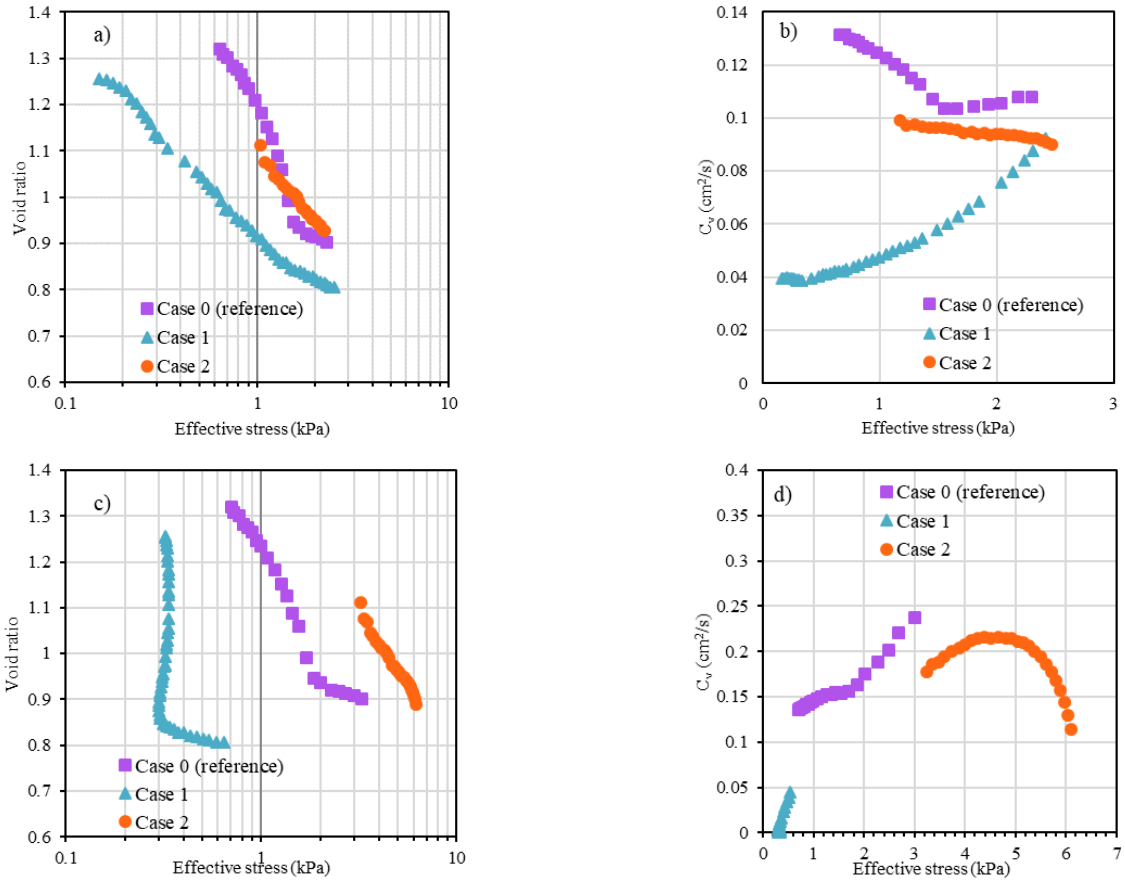

Fig. 10 Variation of the void ratio and coefficient of consolidation cv as a function of effective stresses, obtained by neglecting the arching effect (a and b) or based on the measured vertical total stresses (c and d) after the end of slurry deposition for Cases 0, 1 and 2, respectively

2019). The non-homogeneity due to the segregation should be more pronounced with a small filling rate. All these indicate that the consolidation curve of Case 1 is more reliable than those of Cases 0 and 2. The void ratio e thus decreases while the consolidation coefficient c_v increases as the effective stress increases. The coefficient of consolidation c_v ranges from 0.04 to 0.13 cm^2/s, which are within the range reported by Saleh-Mbemba and Aubertin (2018) who showed that c_v varies from 0.09 to 0.19 cm^2/s for the same tailings with a solid content of 70%.

Generally, similar trends can be observed for the variation of the void ratio (Fig. 10(c)) and coefficient of consolidation cv (Fig. 10(d)) as a function of the effective stress based on the measured vertical total stress and PWP for Case 1. The void ratio decreases while the coefficient of consolidation cv increases as the measured effective stress increases. The differences between the estimated (Figure 10(a)) and measured (Fig. 10(c)) effective stresses indicate that significant arching also occurred in Case 1. When the filling rate is small (Cases 0 and 2), the reliability of the measured effective stresses is significantly low due to the problem of stress shielding effect. The results of Cases 0 and 2 shown in Figure 10d are discussable. More experimental works with reliable measurements of total stresses or more works with standard oedometer consolidations tests are necessary.

5. Discussion

In this paper, a series of column backfilling tests were conducted to investigate the self-weight consolidation characteristics of a slurried backfill during and after the deposition. Compared to most previous laboratory tests, the evolution of PWP, horizontal and vertical total stresses, and settlement in the slurried backfill during and after the deposition were measured simultaneously. The void ratio and coefficient of consolidation were calculated as a function of the vertical effective stress. These results provide an overall view on the self-weight consolidation characteristics of the slurried backfill during and after the deposition, which can be useful for the design of barricades and tailings placement in tailings storage facilities. However, the laboratory tests and results interpretation contain some limitations. For instance, the backfill was prepared without cement because the cement hydration may damage the PWP and stress sensors. The results are thus only valid for uncemented backfill. In practice, cemented backfill is commonly used. Cement hydration can significantly influence the evolution of PWP and total stresses in cemented paste backfill (Helinski *et al.* 2007; Wood *et al.* 2016). It is usually accompanied by the consumption of pore water, resulting in a reduction of PWP and total stresses (Helinski *et al.* 2007; Doherty and Wood 2016). The neglect of cement hydration leads to a

Fig. 11 Accumulation of denser backfill on the cages and top face of the vertical stress sensor near the center of the column

conservative barricade design. However, the decrease of the permeability associated with the cement hydration has effect to slow down the drainage and consolidation. More work is required to conduct column backfilling tests with cemented paste backfill in the future.

In Figs. 4 to 8, one observes an unexpected increase of the vertical total stress after the end of slurry deposition. It even exceeded the iso-geostatic overburden pressure. This can be probably attributed to a phenomenon well-known as the stress shielding effect associated with the presence of stress sensors (Selig 1980). The embedded stiff sensor in the slurried backfill tends to disturb the actual stress field and leads to a stress concentration towards the stiff sensor (Selig 1980; Clayton and Bica 1993; Talesnick 2005; Berthoz *et al.* 2013). This is clearly seen by a picture that shows accumulation of heavy settled backfill over the cages and top face of the vertical total stress sensor (Figure 11). Due to the presence of stiff cage and sensor, the free settlement of tailings particles is impeded above the cages and stiff face of the vertical stress sensor. This results in accumulation of densified backfill near the top surface. The stress shielding effect along with the densified backfill lead to increased and high vertical total stress on the top surface of the vertical stress sensor near the center of the column. More work is required to overcome this problem in the future. But this limitation also illustrates the advantages of laboratory tests compared to field measurements, where there exist a number of uncertainties and the unexpected increase of total stresses can either be interpreted as a problem of stress shielding effect or the results of rock wall closure associated with neighboring excavations or rock creep (e.g., Sobhi and Li 2017, Pagé *et al.* 2019, Qi and Fourie 2019, Wang *et al.* 2019, 2021).

The settled backfill was assumed to be homogeneous when the consolidation parameters were estimated from the measured PWP, total stresses, and settlement. This assumption is not representative because the drainage and consolidation during and after the slurry deposition can result in non-homogeneous backfill. The lower part of the backfill can probably be denser with more coarse particles than the upper part of the backfill. More work is required to consider the non-homogeneous of the settled backfill in the estimation of the consolidation parameters in the future.

Finally, it should be noted that the drainage and consolidation in this study are one-dimensional in the vertical direction. This condition can be representative for mine stope with impervious surrounding rock mass and barricade. In practice, horizontal drainage can take place when the rock walls and/or barricades are permeable. In such cases, laboratory tests can help to better understand the effects of each individual influencing parameter on the PWP and stresses than field measurements. The test results can then be used to validate or calibrate a numerical model. The calibrated and validated numerical model can then be used to handle a problem with more general conditions, including 3D field conditions. More work is still required to investigate the drainage and consolidation of mine backfill under three dimensional conditions.

6. Conclusions

This paper presents a series of column backfilling tests to investigate the evolution of the PWP, total stresses and settlement during and after the deposition. Several consolidation parameters were obtained with the measured results. The main conclusions are summarized as follows:

During the deposition, the PWP, horizontal and vertical total stresses increase at the same rate and equal to the iso-geostatic overburden pressure when the filling rate is higher than 0.18 m/h. The backfill behaves like a liquid with little generation of effective stresses. These results correspond well to the field measurements conducted by Thompson *et al.* (2012). The PWP and horizontal total stresses reach peak value at the end of deposition. After then, they decrease with time due to the drainage and consolidation. The critical moment for barricade design is thus at the end of deposition. High filling rate and/or high solid content lead to high PWP and horizontal total stresses at the end of deposition, which should be avoided in backfilling operation.

The settlement of settled backfill after the end of slurry deposition can generally be divided into two stages. The first one is much faster than the second one. The duration and final settlement of the settled backfill increase as the solid content decreases. It is thus advantageous to use thickened backfill to accelerate the settlement process and reduce the settlement. The final settlement after the end of slurry deposition is related to the solid content, not to the filling rate.

The void ratio and consolidation coefficient have been approximately estimated as a function of effective stress. The results show that the value of c_v slightly increases with the effective stress. Its value ranges from 0.04 to 0.13 cm^2/s, which is consistent with the results reported by Saleh-Mbemba and Aubertin (2018) for the same tailings with a solid content of 70%.

It is interesting to note that the variation of coefficient of consolidation c_v with effective stress can be divided into three stages. When the effective stress is very small, the coefficient of consolidation c_v increases with the effective

stress. When the effective stress exceeds a certain value, but still relatively small, the coefficient of consolidation c_v increase slightly with the effective stress. When the effective stress is large enough, the coefficient of consolidation c_v tends to decrease. More work is still necessary to obtain a better estimation of the vertical effective stress to increase the reliability of the estimated parameters.

Acknowledgments

The authors would like to acknowledge the financial support from the Natural Sciences and Engineering Research Council of Canada (NSERC 402318), Institut de recherche Robert-Sauvé en santé et en sécurité du travail (IRSST 2013-0029), Fonds de recherche du Québec – Nature et Technologies (2015-MI-191676), Mitacs Elevate Postdoctoral Fellowship (IT12572), and industrial partners of the Research Institute on Mines and the Environment (RIME UQAT-Polytechnique; http://rime-irme.ca/).

References

Askew, J.E., McCarthy, P.L. and Fitzerald, D.J. (1978), "Backfill research for pillar extraction at ZC/NBHC", *Proceedings of the 12th Canadian Rock Mechanics Symp*osium, Sudbury, Canada, May.

Aubertin, M., Bussière, B. and Bernier, L. (2002), *Environnement et Gestion des Rejets Miniers*, Presses Internationales de Polytechnique, Montreal, Quebec, Canada.

Aubertin, M., Li, L., Arnoldi, S., Belem, T., Bussière, B., Benzaazoua, M. and Simon, R. (2003), "Interaction between backfill and rock mass in narrow stopes", *Proceedings of the Soil and Rock America 2003: 12th Panamerican Conference on Soil Mechanics and Geotechnical Engineering and 39th U.S. Rock Mechanics Symposium,* Boston, Massachusetts, U.S.A., June

Belem, T., Harvey, A., Simon, R. and Aubertin, M. (2004), "Measurement of internal pressures of a gold mine pastefill during and after the stope backfilling." *Proceedings of the 5th International Symposium on Ground Support in Mining and Underground Construction*, Perth, Australia, September.

Benzaazoua, M., Belem, T. and Jolette, D. (2000), "Investigation de la stabilité chimique et son impact sur la résistance mécanique des remblais cimentés." Report IRSST, IRSST ed., R-260: 2000, pp 158 + Annexes.

Berthoz, N., Branque, D., Wong, H. and Subrin, D. (2013), "Stress measurement in partially saturated soils and its application to physical modeling of tunnel excavation", *Can. Geotech. J.,* **50**(10), 1077-1087. https://doi.org/10.1139/cgj-2013-0154.

Bloss, M.L. and Chen, J. (1998), "Drainage research at Mount Isa Mines Limited 1992–1997", *Proceedings of the 6th International Symposium on Mining with Backfill*, Brisbane, Australia.

Boudrias, G. (2018), "Évaluation numérique et expérimentale du drainage et de la consolidation de résidus miniers à proximité d'une inclusion de roches stériles (in French)", Master Dissertation, École Polytechnique de Montréal, Montréal, Canada.

Bussière, B. (2007), "Colloquium (2004): Hydro-geotechnical properties of hard rock tailings from metal mines and emerging geo-environmental disposal approaches", *Can. Geotech. J.*, **44**(9), 1019-1052. https://doi.org/10.1139/T07-040.

Cao, S., Yilmaz, E. and Song, W. (2018), "Evaluation of viscosity, strength and microstructural properties of cemented tailings backfill", *Minerals*, **8**(8), 352. https://doi.org/10.3390/min8080352.

Cao, S., Xue, G.L., Yilmaz, E. and Yin, Z.Y. (2021), "Assessment of rheological and sedimentation characteristics of fresh cemented tailings backfill slurry", *Int. J. Min. Reclam. Env.*, **35**(5), 319-335. https://doi.org/10.1080/17480930.2020.1826092.

Chen, Q.S., Zhang, Q.L., Qi, C.C., Fourie, A. and Xiao, C.C. (2018), "Recycling phosphogypsum and construction demolition waste for cemented paste backfill and its environmental impact", *J. Clean. Prod.*, **186**, 418-429. https://doi.org/10.1016/j.jclepro.2018.03.131.

Clayton, C.R.I. and Bica, A.V.D. (1993), "The design of diaphragm-type boundary total stress cells", *Geotechnique*, **43**(4), 523–535. https://doi.org/10.1680/geot.1993.43.4.523.

Cui, L. and Fall, M. (2017), "Multiphysics modeling of arching effects in fill mass", *Comput. Geotech.,* **83**, 114-131. https://doi.org/10.1016/j.compgeo.2016.10.021.

Darling, P. (2011), *SME Mining Engineering Handbook,* 3rd Edition, Society for Mining, Metallurgy, and Exploration, Inc.

Dalcé, J. B., Li, L. and Yang, P.Y. (2019), "Experimental study of uniaxial compressive strength (UCS) distribution of hydraulic backfill associated with segregation", *Minerals*, **9**, 147. https://doi.org/10.3390/min9030147.

Doherty, J.P., Hasan, A., Suazo, G.H. and Fourie, A. (2015), "Investigation of some controllable factors that impact the stress state in cemented paste backfill", *Can. Geotech. J.*, **52**(12), 1901-1912. https://doi.org/10.1139/cgj-2014-0321.

Doherty, J.P. and Wood, D.M. (2016), "Back analysis of the Kanowna Belle stope filling case history", *Comput. Geotech.*, **76**, 201-211. https://doi.org/10.1016/j.compgeo.2016.03.009.

El Mkadmi, N., Aubertin, M. and Li, L. (2013), "Effect of drainage and sequential filling on the behavior of backfill in mine stopes", *Can. Geotech. J.*, **51**(1), 1–15. https://doi.org/10.1139/cgj-2012-0462.

Essayad, K. (2015), "Development of Experimental Protocols for the Characterization of Saturated and Unsaturated Tailings Consolidation from Compression Tests in Columns", Master Dissertation, École Polytechnique de Montréal, Montréal, Canada (in French).

Essayad, K. and Aubertin, M. (2021), "Consolidation of hard rock tailings under positive and negative pore-water pressures: testing procedures and experimental results", *Can. Geotech. J.*, **58**(1), 49-65. https://doi.org/10.1139/cgj-2019-0594.

Fahey, M., Helinski, M. and Fourie, A. (2010), "Consolidation in accreting sediments: Gibson's solution applied to backfilling of mine stopes", *Géotechnique,* **60**(11), 877-882. https://doi.org/10.1680/geot.9.P.078.

Falaknaz, N., Aubertin, M. and Li, L. (2015a), "Evaluation of the stress state in two adjacent backfilled stopes within an elasto-plastic rock mass", *Geotech. Geol. Eng.*, 1-24. https://doi.org/10.1007/s10706-015-9868-6.

Falaknaz, N., Aubertin, M. and Li, L. (2015b), "Numerical analyses of the stress distribution in two neighbouring backfilled stopes", *Int. J. Geomech.*, **15**(6), 1019-1052. https://doi.org/10.1061/(ASCE)GM.1943-5622.0000466.

Falaknaz, N., Aubertin, M. and Li, L. (2015c), "Numerical investigation of the geomechanical response of adjacent backfilled stopes", *Can. Geotech. J.,* **52**(10), 1507-1525. https://doi.org/10.1139/cgj-2014-0056.

Fall, M., Benzaazoua, M. and Ouellet, S. (2004), "Effect of tailings properties on paste backfill performance", *Proceedings 8th International Symposium on Mining with Backfill*, Beijing, China, September.

Fall, M., Belem, T. and Benzaazoua, M. (2005), "The compressive and tensile properties of underground paste backfill", *Proceedings of the 58th Canadian Geotechnical and 6th Joint IAH-CNC and CGS Groundwater Specialty Conferences*, Saskatoon, Canada, September.

Grice, T. (1998), "Stability of hydraulic backfill barricades", *Proceedings of the 6th International Symposium of Mining and Backfill*, Brisbane, Australia.

Hassani, F. and Archibal, J. (1998), *Mine Backfill (CD-ROM),* Canadian Institute of Mine, Metallurgy and Petroleum, Canada.

Helinski, M. and Grice, A.G. (2007), "Water management in hydraulic fill operations", *Proceedings of the 9th International Symposium in Mining with Backfill*, Montreal, Quebec, Canada.

Helinski, M., Fourie, A., Fahey, M. and Ismail, M. (2007), "Assessment of the self-desiccation process in cemented mine backfills", *Can. Geotech. J.,* **44**(10), 1148–1156. https://doi.org/10.1139/T07-051.

Helinski, M., Fahey, M. and Fourie, A. (2011), "Behaviour of cemented paste backfill in two mine stopes measurements and modelling", *J. Geotech. Geoenviron. Eng.*, **137**(2), 171-182. https://doi.org/10.1061/(ASCE)GT.1943-5606.0000418.

Huynh, L., Beattie, D.A., Fornasiero, D. and Ralston, J. (2006), "Effect of polyphosphate and naphthalene sulfonate formaldehyde condensate on the rheological properties of dewatered tailings and cemented paste backfill", *Miner. Eng*, **19**(1), 28-36. ttps://doi.org/10.1016/j.mineng.2005.05.001.

Jahanbakhshzadeh, A., Aubertin, M. and Li, L. (2017), "A new analytical solution for the stress state in inclined backfilled mine stopes", *Geotech. Geol. Eng.*, **35**(3), 1151-1167. https://doi.org/10.1007/s10706-017-0171-6.

Jahanbakhshzadeh, A., Aubertin, M. and Li, L. (2018a), "Three-dimensional stress state in inclined backfilled stopes obtained from numerical simulations and new closed-form solution", *Can. Geotech. J.*, **55**(6), 810-828. https://doi.org/10.1139/cgj-2016-0385.

Jahanbakhshzadeh, A., Aubertin, M. and Li, L. (2018b), "Analysis of the stress distribution in inclined backfilled stopes using closed-form solutions and numerical simulations", *Geotech. Geol. Eng*., **36**(2), 1011-1036. https://doi.org/10.1007/s10706-017-0371-0.

Jaouhar, E.M. and Li, L. (2019), "Effect of drainage and consolidation on the pore water pressures and total stresses within backfilled stopes and on barricades", *Adv. Civ. Eng.,* **2019**, 1802130. https://doi.org/10.1155/2019/1802130.

Jaouhar, E.M., Li, L. and Aubertin, M. (2018), "An analytical solution for estimating the stresses in vertical backfilled stopes based on a circular arc distribution", *Geomech. Eng.*, **15**(3), 889-898. https://doi.org/10.12989/gae.2018.15.3.889.

Kesimal, A., Yilmaz, E. and Ercikdi, B. (2004), "Evaluation of paste backfill test results obtained from different size slumps with varying cement contents for sulphur-rich mill tailings", *Cement Concrete Res.*, **34**(10), 1817-1822.

Knutsson, S. (1981), "Stresses in the hydraulic backfill from analytical calculations and in situ measurements", *Proceedings of the Conference on Application of Rock Mechanical to Cut and Fill Mining, Institution of Mining and Metallurgy*, London, .U.K.

Komurlu, E. and Kesimal, A. (2015), "Sulfide-rich mine tailings usage for short-term support purposes: An experimental study on paste backfill barricades", *Geomech. Eng*., **9**(2), 195-205. http://doi.org/10.12989/gae.2015.9.2.195.

Komurlu, E., Kesimal, A. and Demir, S. (2016), "Experimental and numerical analyses on determination of indirect (splitting) tensile strength of cemented paste backfill materials under different loading apparatus", *Geomech. Eng.,* **10**(6), 775-791. http://doi.org/10.12989/gae.2016.10.6.775

Li, L., Aubertin, M. and Belem, T. (2005), "Formulation of a three-dimensional analytical solution to evaluate stresses in backfilled vertical narrow openings", *Can. Geotech. J.*, **42**(6), 1705-1717. https://doi.org/10.1139/t05-084.

Li, L. and Aubertin, M. (2008), "An improved analytical solution to estimate the stress state in sub-vertical backfilled stopes", *Can. Geotech. J.*, **45**(10), 1487-1496. https://doi.org/10.1139/T08-060.

Li, L. and Aubertin, M. (2009), "A three-dimensional analysis of the total and effective stresses in submerged backfilled stopes", *Geotech. Geol. Eng.*, **27**(4), 559-569. https://doi.org/10.1007/s10706-009-9257-0.

Li, L. and Aubertin, M. (2010), "An analytical solution for the nonlinear distribution of effective and total stresses in vertical backfilled stopes", *Geomech. Geoeng.*, **5**(4), 237-245. https://doi.org/10.1080/17486025.2010.497871.

Li, L., Alvarez, I.C. and Aubertin, J.D. (2013), "Self-weight consolidation of a slurried deposition: Tests and interpretation", *Int. J. Geotech. Eng.*, **7**(2), 205-213. https://doi.org/10.1179/1938636213Z.00000000016.

Li, L., Aubertin, J.D. and Dubé, J.S. (2014), "Stress distribution in a cohesionless backfill poured in a silo", *Open Civ. Eng. J.*, **8**(1), 1-8. https://doi.org/10.2174/1874149501408010001

Pagé, P., Li, L., Yang, P. and Simon, R. (2019), "Numerical investigation of the stability of a base-exposed sill mat made of cemented backfill", *Int. J. Rock Mech. Min. Sci.*, **114**, 195-207. https://doi.org/10.1016/j.ijrmms.2018.10.008.

Pedroni, L. (2011), "Étude expérimentale et numérique de la sédimentation et de la consolidation des boues de traitement des eaux acides", Ph.D. Dissertation, École Polytechnique de Montréal, Montreal, Canada.

Pirapakaran, K. and Sivakugan, N. (2007a), "Arching within hydraulic fill stopes", *Geotech. Geol. Eng.*, **25**(1), 25-35. https://doi.org/10.1007/s10706-006-0003-6.

Pirapakaran, K. and Sivakugan, N. (2007b), "A laboratory model to study arching within a hydraulic fill stope", *Geotech. Test. J.*, **30**(6), 1-8. https://doi.org/10.1520/GTJ100653.

Qi, C.C. and Fourie, A. (2019), "Numerical investigation of the stress distribution in backfilled stopes considering creep behaviour of rock mass", *Rock. Mech. Rock. Eng*., **52**(9), 3353-3371. https://doi.org/10.1007/s00603-019-01781-0.

Qin, J.H., Zheng, J. and Li, L. (2021b), "Experimental study of the shrinkage behavior of cemented paste backfill", *J. Rock. Mech. Geotech*., **13**(3), 545-554. https://doi.org/10.1016/j.jrmge.2021.01.005.

Qin, J.H., Zheng, J. and Li, L. (2021a), "An analytical solution to estimate the settlement of tailings or backfill slurry by considering the sedimentation and consolidation", *Int. J. Min. Sci. Technol*., **31**(3), 463-471. https://doi.org/10.1016/j.ijmst.2021.02.004.

Saleh-Mbemba, F. and Aubertin, M. (2018), "Characterization of self-weight consolidation of fine-grained mine tailings using moisture sensors", *Geotech. Test. J.*, **41**(3), 543-554. https://doi.org/10.1520/GTJ20170035.

Selig, E.T. (1980), "Soil stress gage calibration", *Geotech. Test. J.*, **3**(4), 153-158. https://doi.org/10.1520/GTJ10912J.

Sivakugan, N. (2008), "Drainage issues and stress developments within hydraulic fill mine stopes", *Aust. J. Civ. Eng*., **5**(1), 61-70. https://doi.org/10.1080/14488353.2008.11463939.

Sivakugan, N., Rankine, R.M., Rankine, K.J. and Rankine, K.S. (2006), "Geotechnical considerations in mine backfilling in Australia", *J. Cleaner Prod*., **14**(12-13), 1168-1175. https://doi.org/10.1016/j.jclepro.2004.06.007.

Sivakugan, N., Widisinghe, S. and Wang, V.Z. (2014), "Vertical stress determination within backfilled mine stopes", *Int. J. Geomech.*, **14**(5), 06014011. https://doi.org/10.1061/(ASCE)GM.1943-5622.0000367.

Sobhi, M.A. and Li, L. (2017), "Numerical investigation of the

stresses in backfilled stopes overlying a sill mat", *J. Rock Mech. Geotech. Eng.*, **9**(3), 490-501. https://doi.org/10.1139/cgj-2016-0165. https://doi.org/10.1016/j.jrmge.2017.01.001.

Sobhi, M.A., Li, L. and Aubertin, M. (2017), "Numerical investigation of earth pressure coefficient along central line of backfilled stopes", *Can. Geotech. J.*, **54**(1), 138-145. https://doi.org/10.1139/cgj-2016-0165.

Take, W. and Valsangkar, A. (2001), "Earth pressures on unyielding retaining walls of narrow backfill width", *Can. Geotech. J.*, **38**(6), 1220-1230. https://doi.org/10.1139/t01-063.

Talesnick, M. (2005), "Measuring soil contact pressure on a solid boundary and quantifying soil arching", *Geotech. Test. J.,* **28**(2), 171-179. https://doi.org/10.1520/GTJ12484.

Thompson, B. D., Bawden, W. F. and Grabinsky, M. W. (2012), "In situ measurements of cemented paste backfill at the Cayeli Mine", *Can. Geotech. J.*, **49**(7), 755-772. https://doi.org/10.1139/t2012-040.

Ting, C.H., Shukla, S.K. and Sivakugan, N. (2011), "Arching in soils applied to inclined mine stopes", *Int. J. Geomech.,* **11**(1), 29-35. https://doi.org/10.1061/(ASCE)GM.1943-5622.0000067.

Ting, C.H., Sivakugan, N. and Shukla, S.K. (2012), "Laboratory simulation of the stresses within inclined stopes", *Geotech. Test. J.,* **35**(2), 280-294. https://doi.org/10.1520/GTJ103693.

Wang, R., Li, L. and Simon, R. (2019), "A model for describing and predicting the creep strain of rocks from the primary to the tertiary stage", *Int. J. Rock Mech. Min. Sci.*, **123**, 104087. https://doi.org/10.1016/j.ijrmms.2019.104087.

Wang, R., Zeng, F. and Li, L. (2021), "Stability analyses of side-exposed backfill considering mine depth and extraction of adjacent stope", *Int. J. Rock Mech. Min. Sci.*, **142**, 104735. https://doi.org/10.1016/j.ijrmms.2021.104735.

Wood, D.M., Doherty, J.P. and Walske, M.L. (2016), "Deposition and selfweight consolidation of a shrinking fill", *Géotechnique Lett.*, **6**(1), 72-76. https://doi.org/10.1680/jgele.15.00142.

Yang, P. Y., Li, L. and Aubertin M. (2016), "Stability analyses of waste rock barricades designed to retain paste backfill", *Int. J. Geomech.*, **17**(3), 04016079. https://doi.org/10.1061/(ASCE)GM.1943-5622.0000740.

Yang, P. Y., and Li, L. (2017), "Evolution of water table and pore-water pressure in stopes with submerged hydraulic fill", *Int. J. Geomech.*, **17**(9), 04017052. https://doi.org/10.1061/(ASCE)GM.1943-5622.0000944.

Zheng, J., Li, L., Mbonimpa, M. and Pabst, T. (2018a), "An analytical solution of Gibson's model for estimating the pore water pressures in accreting deposition of slurried material under one-dimensional self-weight consolidation. Part I: Pervious base", *Ind. Geotech. J.*, **48**(1), 72-83. https://doi.org/10.1007/s40098-017-0234-x.

Zheng, J., Li, L., Mbonimpa, M. and Pabst, T. (2018b), "An analytical solution of Gibson's model for estimating pore water pressures in accreting deposition of slurried material under one-dimensional self-weight consolidation. Part II: Impervious base", *Ind. Geotech. J.*, **48**(1), 188-195. https://doi.org/10.1007/s40098-017-0234-x.

Zheng, J., Li, L. and Li, Y.C. (2019), "Total and effective stresses in backfilled stopes during the fill placement on a pervious base for barricade design", *Minerals*, **9**(1), 38. https://doi.org/10.3390/min9010038.

Zheng, J. and Li, L. (2020a), "Experimental study of the "short-term" pressures of uncemented paste backfill with different solid contents for barricade design", *J. Clean. Prod.*, **275**, 123068. https://doi.org/10.1016/j.jclepro.2020.123068.

Zheng, J., Li, L., and Li, Y.C. (2020b), "A solution to estimate the total and effective stresses in backfilled stopes with an impervious base during the filling operation of cohesionless backfill. *Int. J. Numer. Anal. Met. Geomech.*, **44**(11), 1570-1586. https://doi.org/10.1002/nag.3079.

CC